Response to Anonymous Referee #1 – Development of iron-mediated molecular chlorine chemistry in GEOS-Chem: model description, evaluation and global atmospheric implication

We are grateful for the feedback and guidance of reviewer. The comments and concerns have been addressed carefully. Exact comments from the reviewer are in black italic type. Our responses (indent and in normal font) and the corresponding edits in the manuscript (indent and in blue) are shown below.

Comments from Anonymous Referee #1:

Chen et al. incorporate an iron-mediated molecular chlorine (Cl_2) formation mechanism into the GEOS-Chem model. They represent the dynamic solubility of iron (Fe) as a function of aerosol acidity, organic complexation, and mineralogical variability. The comparisons indicate that this newly implemented mechanism significantly improves the model's performance in simulating Cl_2 concentrations and substantially alters the global distribution of atmospheric oxidative capacity and subsequent fine particulate matter loadings. The manuscript is well-structured, the methodology is explicitly described, and the model evaluation is logically sound. The scope of this investigation is suitable for Atmospheric Chemistry and Physics. I recommend publication after the authors address the following questions.

Response in general: We thank the reviewer for the supportive and constructive suggestions.

Major question:

1. Lines 127-128: Please elaborate on the physical justification for mapping dust and non-dust Fe to the properties of fine-mode dust and hydrophilic/hydrophobic black carbon, respectively.

Response 1: Thanks for this comment. We assigned dust and non-dust Fe to different host templates by incorporating established methodologies from previous literature and considering their distinct emission sources and atmospheric transport characteristics.

Since the Fe(III)-mediated chlorine chemistry is primarily constrained to fine particles (Chen et al., 2024), herein we focus on the fine-mode tracers associated with the IMC mechanism. For dust Fe, the fine-mode dust Fe tracers follow the physical properties of the DST1 template (with a diameter < 2μm), including density and dry/wet deposition parameters. This is because dust-derived Fe is physically associated with mineral dust particles, and its atmospheric transport and removal should therefore be consistent with the corresponding fine-dust aerosol host. For non-dust Fe, the properties settings follow the methodology of Hamilton et al. (2019), in which fine-mode Fe from fires and anthropogenic combustion is assumed to have BC-like physical properties. This assumption is reasonable since non-dust Fe is mainly associated with combustion sources and is commonly co-emitted or mixed with carbonaceous aerosols such as BC during atmospheric transport. Accordingly, we assign non-dust Fe (including soluble and insoluble Fe) the physical properties of the corresponding BC (including hydrophilic and hydrophobic BC) species in GEOS-Chem. This treatment ensures that the simulated

Fe tracers undergo more physically reasonable atmospheric transport and scavenging processes. We have added the relevant details in the revised manuscript, as below.

Page 4 Line 129-130 in the revised manuscript: "Since the Fe(III)-mediated chlorine chemistry is primarily constrained to fine particles (Chen et al., 2024), eight new iron-bearing tracers associated with the IMC mechanism are introduced into the model."

Page 4 Line 139-144 in the revised manuscript: "In addition, each Fe tracer is assigned specific physical proxy properties to represent its atmospheric behaviors. Specifically, fine dust Fe follows the physical characteristics of fine-mode dust (DST1), including its prescribed density and deposition parameters. For non-dust Fe, we adopt the physical characteristics of black carbon, as these iron species are typically co-emitted and internally mixed with carbonaceous aerosols. Soluble and insoluble non-dust Fe is further mapped to hydrophilic and hydrophobic host species, respectively. This treatment ensures that the simulated Fe tracers undergo more physically reasonable atmospheric transport and scavenging processes."

2. Line 165: In Equation 4, the formulation relies on the term Max[SOA]. Please explicitly define this term. Does it represent a global spatial maximum or a temporal maximum at a specific grid box?

Response 2: Thanks for this comment. Max[SOA] represents the global maximum SOA concentration diagnosed from the model SOA field, rather than a temporal maximum at a specific grid box. It is used as a fixed normalization constant to scale the SOA-dependent oxalate proxy in Eq.(4) following Hamilton et al. (2019) and Scanza et al. (2018). We have clarified this definition in the revised manuscript, as below.

Page 5 Line 185-186 in the revised manuscript: "Max[SOA] denotes the global maximum SOA concentration diagnosed from the standard simulation."

3. Figure 1(a): The global distribution shows uncharacteristically high Fe concentrations compared to observations over southern South America. What is the primary emission source driving these high values in the model? If this is attributed to biomass burning, the low solubility shown in Figure 1(b) contradicts the characteristically high initial solubility of biomass-burning Fe.

Response 3: To identify the source responsible for the relatively high Fe concentrations over southern South America, we performed a source-resolved Fe attribution simulation. As shown in Fig. R1, the enhanced Fe concentrations in this region are dominated by dust-derived Fe, rather than biomass-burning Fe.

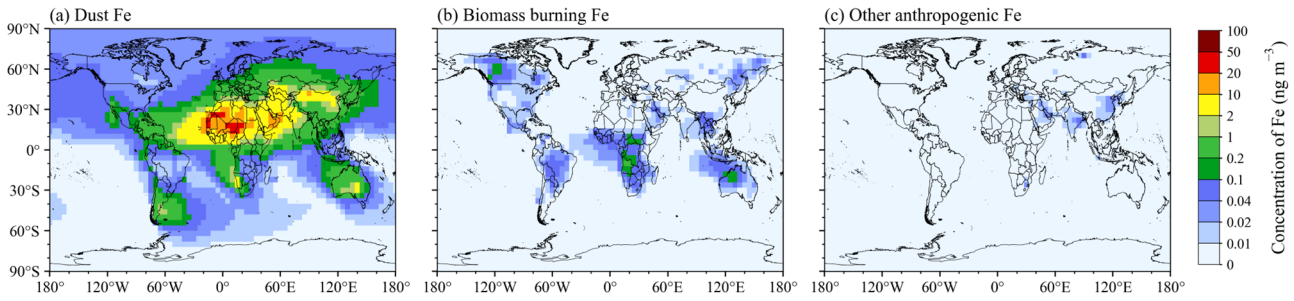

Figure R1. Spatial distributions of annual mean aerosol Fe concentrations contributed by (a) dust, (b) biomass burning, and (c) other anthropogenic sources.

In particular, this region is located close to Patagonia desert, which has been identified as one of the major dust source regions in the Southern Hemisphere (Gassó and Stein, 2007; Johnson et al., 2010; Paparazzo et al., 2018; Demasy et al., 2024). Recent source-attribution results from the AeroCom-III/DUSA multi-model experiments also indicate that Patagonia is an important contributor to southern hemisphere atmospheric dust loading (Kim et al., 2024). Therefore, the high Fe concentrations simulated over southern South America are more consistent with strong contributions from Patagonian dust emissions. Fe in this region is mainly associated with mineral dust which largely present in relatively insoluble mineral forms such as hematite, illite, and smectite. In addition, the region is close to the dust source, where atmospheric aging processes that enhance Fe solubility, including acid processing and organic complexation, are relatively limited. As a result, Fe exhibits a generally low solubility in this area. We have added Fig. R1 to the revised supplementary material (as Fig. S3) and incorporated relevant discussions into the revised manuscript, as below.

Page 7 Line 258-261 in the revised manuscript: "A localized enhancement is also simulated over southern South America, mainly reflecting the contribution of dust-derived Fe from the Patagonian dust source region (Fig. S3), which has been identified as an important dust source in the Southern Hemisphere (Demasy et al., 2024; Gassó and Stein, 2007; Paparazzo et al., 2018)."

Page 8 Line 273-275 in the revised manuscript: "A similar feature is found over southern South America, where the enhanced Fe is mainly associated with freshly emitted Patagonian dust. The low solubility in this region is therefore consistent with the dominance of relatively insoluble mineral Fe phases and the limited atmospheric aging near the dust source."

4. Figure 1(b): How do the authors explain the high modeled Fe solubility in the mid-to-high latitudes of North America compared to the lower solubility in East Asia? Given that both regions experience frequent open biomass burning, which should emit highly soluble Fe, this regional discrepancy requires further clarification.

Response 4: Thanks for this comment. As shown by the Fe source-apportionment results presented in Response 3 (Fig. R1), the regional contrast in Fe solubility is closely related to differences in the dominant Fe

sources. The relatively high Fe solubility over the mid-to-high latitudes of North America is associated with the stronger contribution of biomass-burning Fe, particularly over boreal fire-influenced regions. Since biomass burning generally emits Fe with higher initial solubility, its larger relative contribution increases the bulk aerosol Fe solubility in this region. In contrast, although open biomass burning also occurs in East Asia, biomass-burning Fe contributes only a minor fraction of the annual mean aerosol Fe burden there. The total Fe concentration over East Asia is instead strongly influenced by mineral dust and other anthropogenic Fe sources, which generally correspond to the low-initial-solubility Fe categories in our model. Previous studies have shown that natural dust from the Taklimakan and Gobi deserts can be transported eastward and southward, supplying dust-derived Fe to East Asia and the Northwest Pacific (Zhu et al., 2025). In addition, anthropogenic fugitive, combustion, and industrial dust emissions are particularly important over East and South Asia (Philip et al., 2017). Consistently, source-apportionment analysis of East Asian outflow aerosols shows that fine-particle Fe is mainly associated with fresh/aged dust and anthropogenic sources such as the steel industry, with dominant Fe-bearing phases including aluminosilicates and Fe-oxide nanoparticles (Bunnell et al., 2025; Sakata et al., 2025). As a result, the soluble Fe signal from biomass burning is diluted by these lower-solubility sources, leading to lower modelled bulk Fe solubility over East Asia than over the mid-to-high latitudes of North America. We have added this clarification in the revised manuscript, as below.

Page 8 Line 277-285 in the revised manuscript: "In addition to atmospheric processing, regional differences in Fe source composition also contribute to the spatial variability of Fe solubility. Although both mid-to-high-latitude North America and East Asia experience frequent open biomass burning, they exhibit distinct Fe solubility patterns. As shown in Fig. S3, the relatively high solubility over northern North America is mainly associated with the stronger contribution of boreal biomass-burning Fe, which is represented with relatively high initial solubility in the model. In East Asia, however, aerosol Fe is mainly from mineral dust transported from the Taklimakan and Gobi deserts, as well as anthropogenic fugitive, combustion, and industrial Fe sources (Philip et al., 2017; Zhu et al., 2025; Bunnell et al., 2025; Sakata et al., 2025), which generally correspond to lower Fe solubility. Therefore, the biomass-burning Fe signal is largely diluted by these larger Fe inputs, leading to lower bulk Fe solubility over East Asia despite the occurrence of biomass burning."

5. Lines 357-359: In NOx-rich regions, the enhanced OH and HO_2 are also contributed by the nighttime $ClNO_2$ chemistry.

Response 5: Thanks for this helpful comment. We have added a discussion in the revised manuscript to acknowledge the contribution of nighttime $ClNO_2$ chemistry to enhanced OH and HO_2 in NO*x*-rich regions, as below.

Page 12 Line 410-412 in the revised manuscript: "This enhancement is also partly contributed by nighttime $ClNO_2$ chemistry, as nocturnal $ClNO_2$ formation followed by morning photolysis provides an additional Cl

radical source, further promoting HO_2 production and subsequent OH regeneration (Liu et al., 2017; Riedel et al., 2014).

6. Lines 390-393: The authors attribute the increase in nitrate in the North China Plain to Cl-initiated OH enhancements. However, Figure S5 shows a concurrent decrease in sulfate in this region. Since elevated OH should accelerate SO_2 oxidation and increase sulfate, please further discuss the contraction.

Response 6: Thanks for this comment. Previous studies have shown that daytime nitrate formation is primarily controlled by the OH-initiated NO_2 oxidation and subsequent gas–particle partitioning (Liu et al., 2020; Wang et al., 2026), the strengthened oxidizing environment accelerates nitrate formation and thereby increases $PM_{2.5}$ mass concentration (Feng et al., 2021; Fu et al., 2020; Zang et al., 2022). In this study, the increase in Cl_2 over the NCP generates Cl radicals through photolysis, which further elevates regional OH levels and accelerates the conversion of NO*x* to nitrate.

In contrast, sulfate formation is jointly influenced by multiple SO_2 oxidation pathways, including gas-phase reactions with OH radicals or stabilized Criegee intermediates, heterogeneous-phase reactions on the surface of particles, and aqueous-phase reactions with dissolved O_3, NO_2, H_2O_2, and organic peroxides, as well as autoxidation catalyzed by transition metals (Liu et al., 2020; Guo et al., 2024; Gao et al., 2024; He et al., 2025). In addition to these conventional pathways, hydroxymethanesulfonate (HMS) formed through the reaction between dissolved SO_2 and HCHO can subsequently be oxidized by aqueous OH radicals to sulfate (Song et al., 2019, Ma et al., 2020, Dovrou et al., 2022). In this study, the enhanced iron-chlorine chemistry simultaneously elevates regional OH levels and promotes HCHO production which further increases the concentration of HMS (as shown in Fig. R2a). On the one hand, this process competitively consumes precursors (SO_2) that would otherwise be available for direct oxidation to sulfate. On the other hand, since HMS is relatively stable under acidic conditions and resistant to oxidation by common aqueous oxidants such as H_2O_2 or O_3 (Dovrou et al., 2022), sulfate production via HMS oxidation may not fully compensate for the suppression of conventional formation routes. Consequently, sulfate concentrations slightly decrease over the NCP despite the enhanced OH levels.

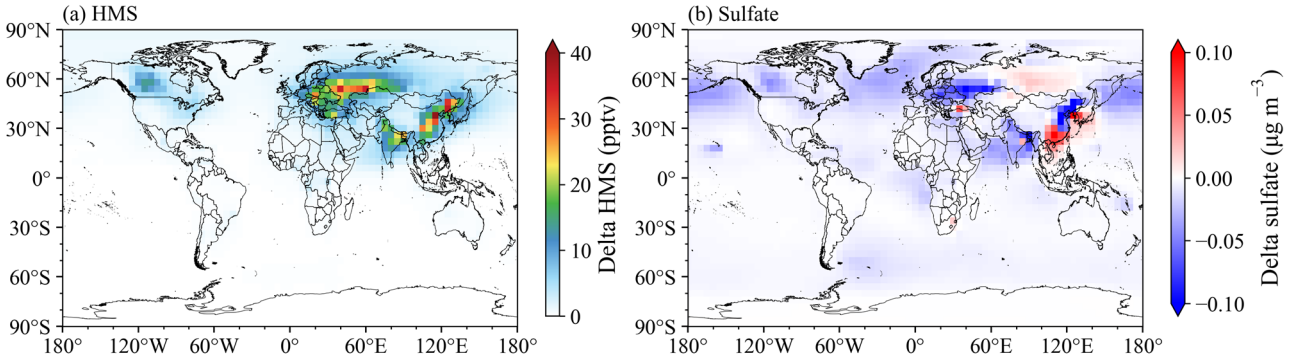

Figure R2. Absolute changes (VarFeS-Base) of annual mean surface concentration of (a) HMS and (b) sulfate.

We have enriched our discussion in the revised manuscript, as below.

Page 13 Line 475-484 in the revised manuscript: "Under conditions of enhanced HO*x* cycling, nitrate and sulfate do not respond uniformly to the IMC mechanism. While nitrate formation is primarily driven by increased OH oxidation (Liu et al., 2020; Wang et al., 2026), sulfate production is governed not only by gas-phase OH oxidation of SO_2 but also by aqueous, heterogeneous, and transition-metal-catalyzed oxidation pathways (Guo et al., 2024; Gao et al., 2024; He et al., 2025). Besides, hydroxymethanesulfonate (HMS) formed through the reaction between dissolved SO_2 and HCHO can subsequently be oxidized by aqueous OH radicals to sulfate (Song et al., 2019, Ma et al., 2020, Dovrou et al., 2022). Though elevated regional OH levels promote HCHO production which further increases the concentration of HMS (Fig.S12), HMS formation may temporarily sequester precursor SO_2, and its subsequent oxidation is likely insufficient to offset the suppression of sulfate formation via direct SO_2 oxidation. Therefore, sulfate concentrations slightly decrease over the NCP despite the enhanced OH levels."

Minor suggestions:

1. Please add a global distribution map for soluble Fe, which could better illustrate the impact of the iron-mediated Cl_2 formation mechanism on Cl_2.

Response 7: We have added a figure to display the global distribution map for soluble Fe in the revised supplementary material, as shown in below.

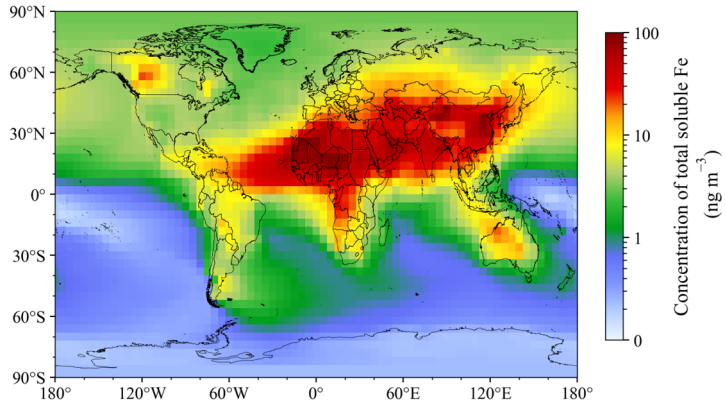

Figure R3. Global distributions of annual mean total soluble Fe concentrations.

We have also added the corresponding description in the revised manuscript, as below.

Page 10 Line 337-339 in the revised manuscript: "Wildfires simultaneously release large amounts of soluble Fe and pCl aerosols from biomass burning within a short period (Tang et al., 2021; Zhang et al., 2022) (the corresponding distribution of soluble Fe concentration is shown in Fig. S6), thereby eliminating precursor limitations on Cl_2 formation processes."

Page 10 Line 351-353 in the revised manuscript: “Although dust-bound Fe possesses lower solubility, the massive total flux ensures that soluble Fe concentrations (43.5 ± 19.0 ng m^{-3}) far above the global mean (7.1 ± 14.8 ng m^{-3}) (Fig. S6), coupled with abundant sea-salt chloride emissions, maintains a stable Cl_2 background in TA.”

References:

Bunnell, Z. B., Sieber, M., Hamilton, D. S., Marsay, C. M., Buck, C. S., Landing, W. M., John, S. G., and Conway, T. M.: The Influence of natural, anthropogenic, and wildfire sources on iron and zinc aerosols delivered to the north Pacific Ocean, Geophys. Res. Lett., 52,doi: 10.1029/2024gl113877, 2025.

Chen, Q., Wang, X., Fu, X., Li, X., Alexander, B., Peng, X., Wang, W., Xia, M., Tan, Y., Gao, J., Chen, J., Mu, Y., Liu, P., and Wang, T.: Impact of molecular chlorine production from aerosol iron photochemistry on atmospheric oxidative capacity in north China, Environ. Sci. Technol., 58, 12585-12597,doi: 10.1021/acs.est.4c02534, 2024.

Demasy, C., Boye, M., Lai, B., Burckel, P., Feng, Y., Losno, R., Borensztajn, S., and Besson, P.: Iron dissolution from Patagonian dust in the Southern Ocean: under present and future conditions, Front. Mar. Sci., 11,doi: 10.3389/fmars.2024.1363088, 2024.

Dovrou, E., Bates, K. H., Moch, J. M., Mickley, L. J., Jacob, D. J., and Keutsch, F. N.: Catalytic role of formaldehyde in particulate matter formation, Proc Natl Acad Sci U S A, 119,doi: 10.1073/pnas.2113265119, 2022.

Feng, T., Bei, N., Zhao, S., Wu, J., Liu, S., Li, X., Liu, L., Wang, R., Zhang, X., Tie, X., and Li, G.: Nitrate debuts as a dominant contributor to particulate pollution in Beijing: Roles of enhanced atmospheric oxidizing capacity and decreased sulfur dioxide emission, Atmos. Environ., 244,doi: 10.1016/j.atmosenv.2020.117995, 2021.

Fu, X., Wang, T., Gao, J., Wang, P., Liu, Y. M., Wang, S. X., Zhao, B., and Xue, L. K.: Persistent heavy winter nitrate pollution driven by increased photochemical oxidants in northern China, Environ. Sci. Technol., 54, 3881-3889,doi: 10.1021/acs.est.9b07248, 2020.

Gassó, S. and Stein, A. F.: Does dust from Patagonia reach the sub-Antarctic Atlantic ocean?, Geophys. Res. Lett., 34,doi: 10.1029/2006gl027693, 2007.

Gao, J., Wang, H., Liu, W., Xu, H., Wei, Y., Tian, X., Feng, Y., Song, S., and Shi, G.: Hydrogen peroxide serves as pivotal fountainhead for aerosol aqueous sulfate formation from a global perspective, Nat. Commun., 15, 4625,doi: 10.1038/s41467-024-48793-1, 2024.

Guo, Z. Y., Lu, K. D., Qiu, P. X., Xu, M. Y., and Guo, Z. B.: Quantifying SO_2 oxidation pathways to atmospheric sulfate using stable sulfur and oxygen isotopes: laboratory simulation and field observation, Atmos. Chem. Phys., 24, 2195-2205,doi: 10.5194/acp-24-2195-2024, 2024.

Hamilton, D., Scanza, R., Yan, F., Guinness, J., Kok, J., Li, L., Liu, X., Rathod, S., Wan, J. S., Wu, M., and Mahowald, N.: Improved methodologies for Earth system modelling of atmospheric soluble iron and observation comparisons using the Mechanism of Intermediate complexity for Modelling Iron (MIMI v1.0), Geosci. Model Dev., 12, 3835-3862,doi: 10.5194/GMD-12-3835-2019, 2019.

He, P. Z., Chi, X. Y., Zhang, B. H., Hua, C., Dao, X., Meng, X. Y., and Ma, T. M.: Exploring the formation of atmospheric nitrate and sulfate based on one-year observations in Beijing, Aerosol Sci. Eng.,doi: 10.1007/s41810-025-00361-w, 2025.

Johnson, M. S., Meskhidze, N., Solmon, F., Gassó, S., Chuang, P. Y., Gaiero, D. M., Yantosca, R. M., Wu, S. L., Wang, Y. X., and Carouge, C.: Modeling dust and soluble iron deposition to the South Atlantic Ocean, J Geophys Res-Atmos, 115,doi: 10.1029/2009jd013311, 2010.

Kim, D., Chin, M., Schuster, G., Yu, H. B., Takemura, T., Tuccella, P., Ginoux, P., Liu, X. H., Shi, Y., Matsui, H., Tsigaridis, K., Bauer, S. E., Kok, J. F., and Schulz, M.: Where dust comes from: Global assessment of dust source aattributions with AeroCom Models, J Geophys Res-Atmos, 129,doi: 10.1029/2024jd041377, 2024.

Liu, P. F., Ye, C., Xue, C. Y., Zhang, C. L., Mu, Y. J., and Sun, X.: Formation mechanisms of atmospheric nitrate and sulfate during the winter haze pollution periods in Beijing: gas-phase, heterogeneous and aqueous-phase chemistry, Atmos. Chem. Phys., 20, 4153-4165,doi: 10.5194/acp-20-4153-2020, 2020.

Ma, T., Furutani, H., Duan, F., Kimoto, T., Jiang, J., Zhang, Q., Xu, X., Wang, Y., Gao, J., Geng, G., Li, M., Song, S., Ma, Y., Che, F., Wang, J., Zhu, L., Huang, T., Toyoda, M., and He, K.: Contribution of hydroxymethanesulfonate (HMS) to severe winter haze in the North China Plain, Atmos. Chem. Phys., 20, 5887-5897,doi: 10.5194/acp-20-5887-2020, 2020.

Paparazzo, F., Crespi-Abril, A., Gonçalves, R., Barbieri, E., Gracia Villalobos, L., Solís, M., and Soria, G.: Patagonian dust as a source of macronutrients in the Southwest Atlantic Ocean, Oceanography, 31, 33-39,doi: 10.5670/oceanog.2018.408, 2018.

Philip, S., Martin, R. V., Snider, G., Weagle, C. L., van Donkelaar, A., Brauer, M., Henze, D. K., Klimont, Z., Venkataraman, C., Guttikunda, S. K., and Zhang, Q.: Anthropogenic fugitive, combustion and industrial dust is a significant, underrepresented fine particulate matter source in global atmospheric models, Environ. Res. Lett., 12, 044018,doi: 10.1088/1748-9326/aa65a4, 2017.

Sakata, K., Takano, S., Matsuki, A., Takeichi, Y., Tanimoto, H., Sakaguchi, A., Kurisu, M., and Takahashi, Y.: Atmospheric chemistry in East Asia determines the iron solubility of aerosol particles supplied to the North Pacific Ocean, Atmos. Chem. Phys., 25, 11087-11107,doi: 10.5194/acp-25-11087-2025, 2025.

Song, S., Gao, M., Xu, W., Sun, Y., Worsnop, D. R., Jayne, J. T., Zhang, Y., Zhu, L., Li, M., Zhou, Z., Cheng, C., Lv, Y., Wang, Y., Peng, W., Xu, X., Lin, N., Wang, Y., Wang, S., Munger, J. W., Jacob, D. J., and McElroy, M. B.: Possible heterogeneous chemistry of hydroxymethanesulfonate (HMS) in northern China winter haze, Atmos. Chem. Phys., 19, 1357-1371,doi: 10.5194/acp-19-1357-2019, 2019.

Scanza, R., Hamilton, D., García-Pando, C. P., Buck, C., Baker, A., and Mahowald, N.: Atmospheric processing of iron in mineral and combustion aerosols: development of an intermediate-complexity mechanism suitable for Earth system models, Atmos. Chem. Phys., 18, 14175-14196,doi: 10.5194/ACP-18-14175-2018, 2018.

Wang, J. Q., Du, X. H., Wen, L., Che, F., Zhang, Y. C., and Gao, J.: Particulate nitrate pollution control in North China Plain and Northeastern United States: A comparison of formation mechanism and its response to gaseous pollutants, Environ. Pollut., 397,doi: 10.1016/j.envpol.2026.127939, 2026.

Zang, H., Zhao, Y., Huo, J. T., Zhao, Q. B., Fu, Q. Y., Duan, Y. S., Shao, J. Y., Huang, C., An, J. Y., Xue, L. K., Li, Z. Y., Li, C. X., and Xiao, H. Y.: High atmospheric oxidation capacity drives wintertime nitrate pollution in the eastern Yangtze River Delta of China, Atmos. Chem. Phys., 22, 4355-4374,doi: 10.5194/acp-22-4355-2022, 2022.

Zhu, H. Z., Liu, Y. M., Yue, M., Feng, S. H., Fu, P. Q., Huang, K., Dong, X. Y., and Wang, M. H.: Trends and drivers of soluble iron deposition from East Asian dust to the Northwest Pacific: a springtime analysis (2001-2017), Atmos. Chem. Phys., 25, 5175-5197,doi: 10.5194/acp-25-5175-2025, 2025.

Response to Anonymous Referee #2 – Development of iron-mediated molecular chlorine chemistry in GEOS-Chem: model description, evaluation and global atmospheric implication

We are grateful for the feedback and guidance of reviewer. The comments and concerns have been addressed carefully. Exact comments from the reviewer are in black italic type. Our responses (indent and in normal font) and the corresponding edits in the manuscript (indent and in blue) are shown below.

Comments from Anonymous Referee #2:

Chen et al. implement an iron-mediated Cl_2 formation pathway into the GEOS-Chem CTM and present the subsequent atmospheric impacts of this scheme on tropospheric chemistry, oxidative environment and PM. The description and evaluation of this scheme is detailed and clear, showing a strong improvement to model bias for Cl_2. I have the following comments and questions for the authors.

Response in general: We are grateful to the reviewer for the very constructive comments and the recognition.

Main comments:

1. Whilst the authors evaluate the model bias changes on Cl_2, there are a number of substantial atmospheric implications from this work which are also of interest, and I believe would help to further evaluate this scheme. There is a number of ways the authors could do this, which would utilise the data they already have and not extend the analysis performed in this paper significantly. They could present tropospheric O_3 burden, global area-weighted-mean OH, methane lifetime and other key whole atmosphere diagnostics for each of the 3 model versions. Additionally with the large changes in surface O_3, all model versions could be compared to readily available observational datasets (such as from GAW or TOAR) to better understand the consequences of the additional Cl chemistry with the context of the base model performance.

Response 1: Thanks for these helpful comments.

(1) Key atmosphere diagnostics for different simulation scenarios.

We calculated several key diagnostics for the three model versions. The tropospheric O_3 burden is 367.9 Tg in the Base scenario, while it decreases to 364.8 and 357.3 Tg in the FixFeS and VarFeS scenarios, respectively. Compared to the Base scenario, the O_3 burden decreases by 2.9% in VarFeS. This reduction is mainly associated with enhanced chlorine activation under the IMC mechanism, which increases Cl radical levels and promotes direct O_3 destruction through Cl–O_3 reactions as well as $ClONO_2$ formation. In addition, perturbations to the RO*x* and HO*x* cycling further affect the global OH abundance. The global surface mean OH concentrations are 8.41×10^5, 8.33×10^5, and 8.16×10^5 molec cm^{-3} for the Base, FixFeS, and VarFeS scenarios, respectively. With the inclusion of the IMC mechanism in the FixFeS and VarFeS scenarios, OH concentrations

decrease accordingly, mainly due to decreases in O_3 weaken primary OH production and conversion of HO*x* to ClO*x*.

A comprehensive assessment of the overall CH_4 lifetime is beyond the scope of the present study, as our main objective is to quantify the effects of the IMC mechanism on atmospheric oxidative capacity and $PM_{2.5}$ formation. Nevertheless, the GEOS-Chem model provides a diagnostic CH_4 lifetime with respect to OH oxidation, which can be used to evaluate the indirect influence of IMC-induced OH perturbations on CH_4 loss. The diagnosed CH_4 lifetime relative to OH are 8.32, 8.39, and 8.54 years for the Base, FixFeS, and VarFeS scenarios, respectively. Compared with the Base case, the IMC mechanism increases this CH_4 lifetime by 0.07 years (0.8%) in FixFeS and by 0.22 years (2.6%) in VarFeS, through its reduction of global OH concentrations. It should be noted that the CH_4 lifetime presented here only reflects the indirect effect of IMC through OH perturbations and does not include the direct CH_4 loss via reaction with Cl radicals. Further analysis of the CH_4 via Cl loss pathway and the full CH_4 chemical budget would help to better constrain the net impact of IMC on methane lifetime. We have added the discussion of tropospheric O_3 burden and global surface mean OH to the revised manuscript, as below.

Page 11 Line 399-400 in the revised manuscript: "With the inclusion of IMC mechanism, the global annual mean surface OH concentrations decreased by 2.5×10^4 atoms cm^{-3}, which corresponds to a 5.7% relative reduction compared to the "Base" scenario."

Page 12 Line 431-433 in the revised manuscript: "Consistent with the widespread decreases in surface O_3 outside high-NO*x* source regions, the tropospheric O_3 burden declines from 367.9 Tg in the Base scenario to 357.3 Tg in the VarFeS scenario, corresponding to a 2.9% reduction."

(2) Surface ozone concentration evaluation

For the surface O_3 evaluation, we used in-situ observations from several publicly available air-quality monitoring datasets, including OpenAQ (https://openaq.org), the China National Environmental Monitoring Centre (http://www.cnemc.cn), the U.S. Environmental Protection Agency (https://www.epa.gov), and the European Environment Agency (https://www.eea.europa.eu/en). Simulation results were sampled at the observation sites and annual mean O_3 concentrations were used for comparation. As shown in Fig. R1, including the IMC mechanism systematically enhances model performance. Specifically, the correlation coefficient increases from 0.64 for Base scenario to 0.65 and 0.72, while the RMSE drops from 15.44 to 14.92 and 13.62 μg m^{-3} and the mean bias decreases from 6.68 to 6.04 and 5.26 μg m^{-3} for FixFeS and VarFeS scenario, respectively. These results indicate that the inclusion of the IMC mechanism improves the model representation of annual mean surface O_3, with the most pronounced improvement obtained in the VarFeS scenario.

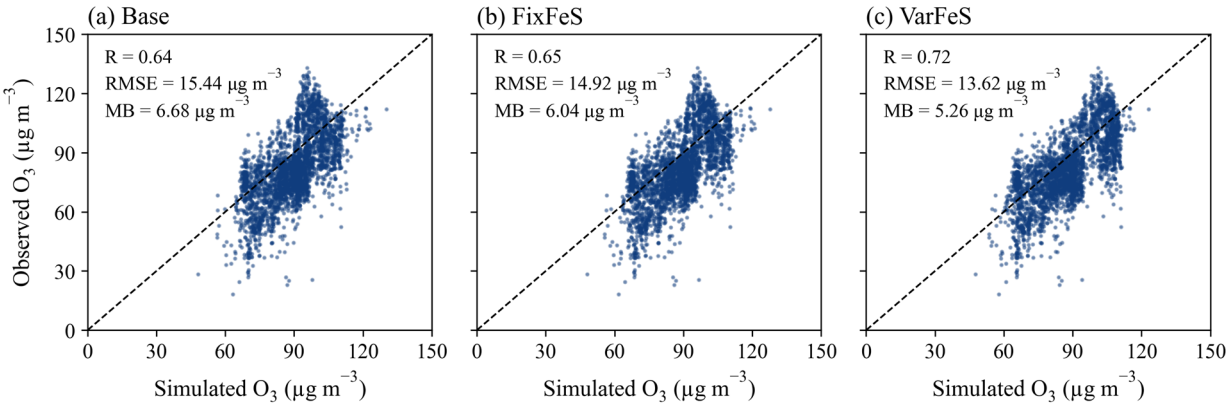

Figure R1. Comparison of observed and simulated annual mean surface O_3 concentrations for the (a) Base, (b) FixFeS, and (c) VarFeS scenarios. The dashed line denotes the 1:1 line. R, RMSE, and MB represent the correlation coefficient, root mean square error, and mean bias, respectively.

We have added a new section, "Text S1: Evaluation of surface O_3 concentrations", to the revised supplementary materials, and the corresponding statement has also been included in the revised manuscript, as below.

Page 12 Line 425-426 in the revised manuscript: "Including the IMC mechanism improves the model representation of surface O_3 relative to the Base scenario (Text S1 in the supplementary Materials), this provides further context for interpreting the simulated O_3 responses."

Page 11 in the revised supplementary materials: "To further assess whether the inclusion of the IMC mechanism affects the model representation of surface ozone, we compared simulated annual mean surface O_3 concentrations with in-situ observations from publicly available air-quality monitoring datasets, including OpenAQ (https://openaq.org), the China National Environmental Monitoring Centre (http://www.cnemc.cn), the U.S. Environmental Protection Agency (https://www.epa.gov), and the European Environment Agency (https://www.eea.europa.eu/en). As shown in Fig. S13, the inclusion of the IMC mechanism improves the model–observation agreement for surface O_3. Specifically, the correlation coefficient increases from 0.64 in the Base simulation to 0.65 and 0.72 in the FixFeS and VarFeS simulations, respectively. Meanwhile, the RMSE decreases from 15.44 μg m^{-3} to 14.92 and 13.62 μg m^{-3}, and the mean bias decreases from 6.68 μg m^{-3} to 6.04 and 5.26 μg m^{-3}, respectively. These results suggest that the including IMC mechanism improves the annual mean model performance, with the most pronounced improvement in the VarFeS scenario."

2. The authors could further explore the effects of this scheme on particulate matter with further discussion on both the areas of increase and decrease and the respective drivers of these.

Response 2: Thanks for this critical comment. We have enriched the discussion regarding the spatial heterogeneity of $PM_{2.5}$ changes in the revised manuscript, as below.

Page 13 Line 453-484 in the revised manuscript: “Including the IMC mechanism significantly reshapes the global AOC by modulating radical cycling, which subsequently exerts a distinct influence on the formation and spatial distribution of fine particulate matter ($PM_{2.5}$) pollution, as shown in Fig. 6.

Spatially, $PM_{2.5}$ enhancements are primarily concentrated in the mid-to-high latitude land areas of the Northern Hemisphere. While slight increases of roughly 0.5% are found in western Europe, northern America, Canada, and parts of the Arctic Ocean, the most pronounced response appears over the NCP, where $PM_{2.5}$ rises by up to 2.5% (+2.2 μg m^{-3}). From the perspective of chemical composition (Fig. S10), the $PM_{2.5}$ enhancement is predominantly driven by nitrate formation. Over the NCP, nitrate rises by 1.9 μg m^{-3}, accompanied by a smaller increase in ammonium (+0.4 μg m^{-3}). This nitrate-dominated response is closely linked to elevated Cl_2 concentrations. Photolysis of Cl_2 generates highly reactive Cl radicals that substantially increase OH levels over the NCP. Since OH radicals are the critical daytime oxidants driving the conversion of nitrogen oxides into nitrate (Liu et al., 2020; Wang et al., 2026), the strengthened oxidizing environment accelerates nitrate formation and thereby increases $PM_{2.5}$ mass concentration. This is consistent with previous studies reporting that increasing AOC significantly contributes to enhanced nitrate and $PM_{2.5}$ concentrations (Feng et al., 2021; Fu et al., 2020; Zang et al., 2022). Importantly, this mechanism is further amplified under wintertime conditions, when stagnant meteorology and elevated precursor emissions coexist. In winter over the NCP, $PM_{2.5}$ increases can reach up to 6.2% (Fig. S11). High NO*x* levels, frequent stagnation, shallow boundary layers, and low-temperature conditions favorable for particulate nitrate stability collectively promote the partitioning of HNO_3 into the particle phase. As a result, nitrate formation is substantially enhanced, leading to a pronounced increase in $PM_{2.5}$ in this region.

In contrast, regions located downwind of the enhanced Cl_2 production zones, as well as adjacent marine areas, exhibit a general decrease in $PM_{2.5}$ concentrations. This reduction is likely attributable to the accelerated oxidation of NO*x* and other precursors near the source regions under strengthened AOC. As NO*x* is more rapidly converted to HNO_3 and subsequently to particulate nitrate, these species undergo earlier deposition and removal, thereby diminishing the reservoir of precursors available for long-range transport and secondary aerosol formation. Consequently, the downwind regions experience lower $PM_{2.5}$ levels. In addition, this decreasing pattern is also consistent with the spatial distribution of sulfate reductions (Fig. S10). Under conditions of enhanced HO*x* cycling, nitrate and sulfate do not respond uniformly to the IMC mechanism. While nitrate formation is strongly driven by increased OH oxidation (Liu et al., 2020; Wang et al., 2026), sulfate production is governed not only by gas-phase OH oxidation of SO_2 but also by aqueous, heterogeneous, and transition-metal-catalyzed oxidation pathways (Guo et al., 2024; Gao et al., 2024; He et al., 2025). Besides, hydroxymethanesulfonate (HMS) formed through the reaction between dissolved SO_2 and HCHO can subsequently be oxidized by aqueous OH radicals to sulfate (Song et al., 2019, Ma et al., 2020, Dovrou et al., 2022). Though elevated regional OH levels promote HCHO production which further increases the concentration of HMS (Fig.S12), HMS formation may temporarily sequester precursor SO_2, and its subsequent

oxidation is likely insufficient to offset the suppression of sulfate formation via direct SO_2 oxidation. Therefore, sulfate concentrations slightly decrease over the NCP despite the enhanced OH levels."

3. For emission inventories, many in GEOS-Chem will cycle the most recent year available if the current year the model is being run in is unavailable. Could the authors specify the emission years for the CEDS inventories as more recent changes (such as to sulfur emission standards for shipping) may not be captured in this study and could have a potential impact on the results presented.

Response 3: Thank you for this insightful comment. The CEDS anthropogenic emissions used in this study are from CEDS v2025-04 (https://doi.org/10.5281/zenodo.15059443) which extends to 2023 and updates shipping fuel sulfur content by incorporating IMO sulfur-content agreements. For our simulations, the corresponding-year CEDS emissions were used directly rather than being cycled from an earlier available year. Therefore, the effect of recent shipping sulfur reductions associated with the IMO 2020 low-sulfur regulation for shipping has been represented in the CEDS emissions as well.

We have clarified the year used for the different inventories in the revised manuscript, as below.

Page 4 Line 124-127 in the revised manuscript: "In this study, anthropogenic non-BB Fe emissions are scaled to anthropogenic primary sulfate emissions from the Community Emissions Data System (CEDS) emission inventory which extends to 2023 and updates shipping fuel sulfur content by incorporating IMO sulfur-content agreements, assuming a fixed mass ratio of 1:30 following previous studies (Chen et al., 2024; Alexander et al., 2009)."

Page 6 Line 231-232 in the revised manuscript: "All emission inputs correspond to the simulation year 2023 except for AEIC aircraft emissions and AFCID, which are based on year 2019 and 2015 due to data availability."

4. The authors have employed a 6-month spin-up period, the atmospheric impacts are substantial and it is more common for such changes (especially concerning O_3) to run for 1 year or more for this spin-up period. Could the authors consider a longer spin-up period to align this more closely with other studies and further settle any changes in longer-lived species.

Response 4: Thanks for your constructive suggestion. To address this concern, we conducted an additional sensitivity simulation with a 1-year spin-up period and compared the O_3 responses induced by the Fe(III)-mediated Cl_2 formation mechanism under the two spin-up settings. As shown in Fig. R2, the absolute O_3 changes between 'VarFeS' and 'Base' scenarios are highly consistent between the 6-month and 1-year spin-up simulations, with the vast majority of regions showing negligible deviations, indicating that the mechanism-induced O_3 perturbation is not sensitive to extending the spin-up period from 6 months to 1 year. Since our study primarily investigates the impacts of iron-mediated Cl_2 formation on relatively short-lived reactive species (e.g., reactive chlorine species, RO_2, HO*x*) and their immediate influence on O_3 and $PM_{2.5}$, we believe the 6-month spin-up duration is acceptable for this study. We appreciate this perspective and will ensure that a longer

spin-up period is implemented in our future work, particularly for studies involving complex cycles of long-lived species.

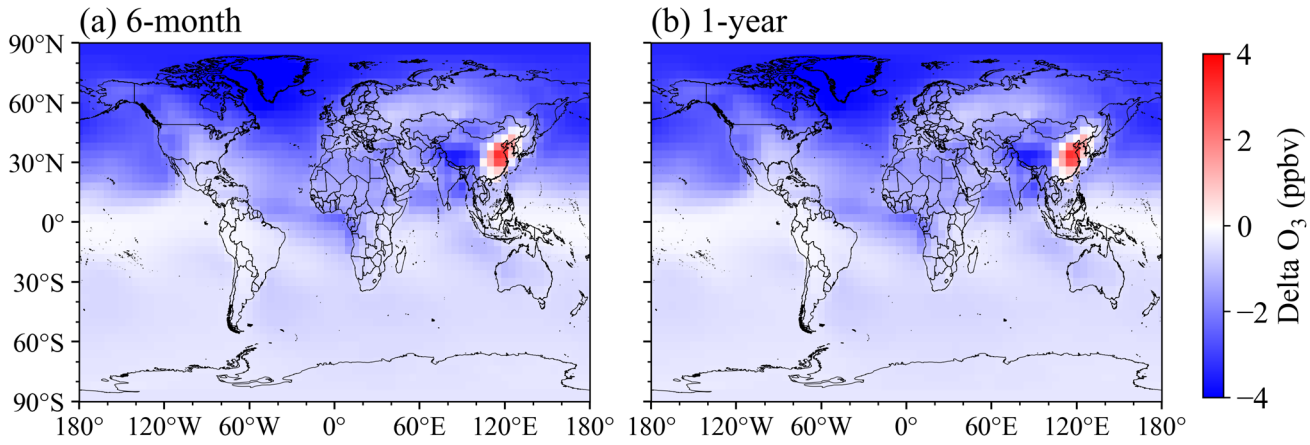

Figure R2. Comparison of absolute changes (VarFeS-Base) of O_3 for (a) 6-month and (b) 1-year spin-up simulations.

Minor/technical comments:

1. When referencing the GEOS-Chem model version (in this case 14.2.3), DOIs are available for all major and minor releases which improve the transparancy and ease of recovering the exact model version used in studies. These are archived on Zenodo and also detaild on the GEOS-Chem readthedocs/wiki.

Response 5: We have added the corresponding DOI citation for GEOS-Chem version 14.2.3 as archived on Zenodo to the revised manuscript, as shown below.

Page 2 Line 71-72 in the revised manuscript: "Global chemical transport model GEOS-Chem (version 14.2.3, https://doi.org/10.5281/zenodo.10246546) was employed to assess the influence of reactive chlorine chemistry on atmospheric processes."

2. The authors have used the reduced vertical grid for this study (47 levels). There have been several issues raised with this (some arising and being fixed by later versions). One that comes to mind is issues with the accuracy of the photolysis in the 47-layer grid, whilst this is most noticeable in the stratosphere, do the authors believe this or any other issues could have any bearing on the results they present?

Response 6: Thanks for raising this important point. We note that a specific 47-layer initialization issue has been reported for GEOS-Chem v14.6.0–v14.6.3 (https://github.com/geoschem/geos-chem/issues/3170), which may affect stratospheric species and photolysis rates. However, our simulations were performed using GEOS-Chem v14.2.3. Since this issue was confirmed not to exist before v14.6.0, our simulations are not affected by it. Regarding the general difference between the 47-layer and 72-layer configurations, the 47-layer grid preserves the native vertical structure through the troposphere and lower stratosphere, with vertical layer

lumping only beginning in the stratosphere, above approximately 70–80 hPa. Therefore, the vertical resolution directly relevant to boundary-layer chemistry, surface O_3, and $PM_{2.5}$ is retained. As the present study focuses primarily on tropospheric and near-surface impacts of Fe(III)-mediated Cl_2 activation, the reduced vertical grid is unlikely to substantially influence our main conclusions. In addition, our conclusions are based on differences between paired simulations using the same vertical grid configuration, namely the Base simulation and the VarFeS simulation including the Fe(III)-mediated Cl_2 activation mechanism. Any systematic influence associated with the reduced vertical grid would thus be largely shared by both simulations and is expected to have a limited impact on the relative changes used to evaluate the chemical mechanism. Accordingly, we have added a new section, "Text S2 Other potential uncertainty analysis.", to the revised supplementary materials to discuss this uncertainty, and the corresponding statement has also been included in the revised manuscript, as below.

Page 9 Line 324 in the revised manuscript: "Other potential uncertainties are discussed in Text S2 in the supplementary materials."

Page 11 in the revised supplementary materials: "Additional uncertainties may also arise from the reduced vertical-grid configuration used in this study. This configuration reduces vertical resolution primarily in the stratosphere and mesosphere, which could introduce uncertainties in stratospheric chemical and transport processes. Since this study focuses mainly on near-surface responses and relative differences between simulations using the same vertical-grid configuration, these uncertainties are expected to have a limited influence on the main conclusions. Future studies specifically targeting stratospheric responses could adopt the full 72-layer configuration or additional sensitivity simulations to further assess the influence of vertical resolution."

3. As this work has involved several changes to the GEOS-Chem source code, it would be good practice for the authors to make these changes publicly available and archived so that results could be replicated. This could be done in a similar version to the public version of GEOS-Chem with the authors using GitHub/Zenodo.

Response 7: Thanks for this comment. The modified GEOS-Chem source-code files associated with Fe dissolution processes and Cl_2 formation mechanisms implemented in this study will be archived on Zenodo and made publicly available upon acceptance.